468 *Inorg. Chem.* **2010**, *49*, 468–475
DOI: 10.1021/ic901408n

Inorganic Chemistry
Article

Stable Silver(I) Hydride Complexes Supported by Diselenophosphate Ligands

C. W. Liu,*,† Hao-Wei Chang,† Bijay Sarkar,† Jean-Yves Saillard,‡ Samia Kahlal,‡ and Ying-Yann Wu§

†*Department of Chemistry, National Dong Hwa University, Hualien, Taiwan 97401, R.O.C.,*
‡*UMR-CNRS, 6226 "Sciences Chimiques de Rennes", Universite' de Rennes 1, 35042 Rennes cedex, France, and* §*Rezwave Technology Inc., His-Chih, Taiwan, 22101, R.O.C.*

Received July 18, 2009

The first stable structure of silver(I) cluster cations $[Ag_8(\mu_4-H)\{Se_2P(OR)_2\}_6]^+$ [R = ^{i}Pr, **1**; Et, **2**] containing Ag(I)-hydride bridges (Ag$-\mu$-H$-$Ag) in *T* symmetry was reported. The clusters having an interstitial hydride were composed of an octanuclear silver core in tetracapped tetrahedral geometry, which was inscribed within a Se_{12} icosahedron represented by six dialkyl diselenophosphate ligands in a tetrametallic-tetraconnective (μ_2, μ_2) bonding mode. The presence of hydride was unequivocally corroborated by both ^{1}H and ^{109}Ag NMR spectroscopies of which a nonet in the ^{1}H NMR spectrum for the hydride resonance coupled with a doublet peak observed in the ^{109}Ag NMR spectrum clearly suggests that eight silver nuclei are equivalent in the NMR time scale and a fast exchange of the positions between the vertex and capping silver atoms in solution must occur. The hypothesis was also supported by a density functional theory (DFT) investigation on a simplified model $[Ag_8(H)(Se_2PH_2)_6]^+$, which confirmed that the Ag_8H cubic core of T_h symmetry may not be formed as it is energetically highly unfavorable (0.67 eV less stable than the *T* structure).

Intoduction

Various catalytic reactions have long been known to proceed through the formation of metal hydrides as a key intermediate.[1] Thus, a hydride on the silver cluster was proposed as a key step in the dehydrogenation of alcohols to ketones catalyzed by Al_2O_3-supported silver clusters.[2,3] In addition, a silver-hydride could be an intermediate in Ag/Al_2O_3-catalyzed C$-$C cross-coupling of secondary alcohols with primary alcohols.[2,3] Although clusters containing silver-transition metal hydride bridges such as [Ru$-$H$-$Ag],[4] [Mo$-$H$-$Ag],[5] [Mn$-$H$-$Ag],[6] [Re$-$H$-$Ag],[7] [Rh$-$H$-$Ag],[8] [Ir$-$H$-$Ag],[9] and [Pt$-$H$-$Ag][10] are well-known, a *stable complex with hydride coordinated solely to the silver is still unknown* due to its unstable nature even though the subvalent silver hydride clusters $(Ag_2H)^+$,[11] and $(Ag_4H)^+$,[12] have been identified in the gas phase. In the literature,[12] $(Ag_4H)^+$ has been postulated as a molecular model for the C$-$C bond coupling of allyl bromide mediated by silver surfaces[13,14] and nanoparticles.[15] Thus, the isolation of compounds with a hydride surrounded entirely by silver atoms may provide better insight into the aforementioned catalytic systems. In addition, the possibilities of activated metal hydrides to act as hydrogen sources, an extremely important issue in hydrogen storage technology, have the study of hydride-entrapment in metal clusters more significant.[16−18]

Birker and his co-workers reported a mixed metal cluster $[Ni^{II}{}_6Ag^{I}{}_8(D\text{-pen})_{12}Cl]^{5-}$ which for the first time revealed a chloride-centered Ag_8 cubic skeleton.[19] The tendency of

*To whom correspondence should be addressed. E-mail: chenwei@mail.ndhu.edu.tw.

(1) Emeléus, H. J.; Sharpe, A. G. *Advances in inorganic chemistry and radiochemistry*; Academic Press: New York, 1965; Vol. *7*.
(2) Shimizu, K.; Sugino, K.; Satsuma, A. *Chem.—Eur. J.* **2009**, *15*, 2341–2351.
(3) Shimizu, K.; Sato, R; Satsuma, A. *Angew. Chem., Int. Ed.* **2009**, *48*, 3982–3986.
(4) Brown, S. S. D.; Salter, I. D.; Sik, V.; Colquhoun, I. J.; McFarlane, W.; Bates, P. A.; Hursthouse, M. B.; Murray, M. *J. Chem. Soc., Dalton Trans.* **1988**, 2177–2185.
(5) Brunner, H.; Mijolovic, D.; Wrackmeyer, B.; Nuber, B. *J. Organomet. Chem.* **1999**, *579*, 298–304.
(6) Carreno, R.; Riera, V.; Ruiz, M. A.; Bois, C.; Jeannin, Y. *Organometallics* **1994**, *13*, 993–1004.
(7) Beringhelli, T.; D'Alfonso, G.; Garavaglia, M. G.; Panigati, M.; Mercandelli, P.; Sironi, A. *Organometallics* **2002**, *21*, 2705–2714.
(8) Bachechi, F.; Ott, J.; Venanzi, L. M. *J. Am. Chem. Soc.* **1985**, *107*, 1760–1761.
(9) Gorol, M.; Mosch-Zanetti, N. C.; Roesky, H. W.; Noltemeyer, M.; Schmidt, H.-G. *Chem. Commun.* **2003**, 46–47.
(10) Albinati, A.; Chaloupka, S.; Demartin, F.; Koetzle, T. F.; Ruegger, H.; Venanzi, L. M.; Wolfer, M. K. *J. Am. Chem. Soc.* **1993**, *115*, 169–175.
(11) Flurer, R. A.; Busch, K. L. *J. Am. Chem. Soc.* **1991**, *113*, 3656–3663.
(12) Khairallah, G. N.; O'Hair, R. A. J. *Angew. Chem., Int. Ed.* **2005**, *44*, 728–731.
(13) Celio, H.; White, J. M. *J. Phys. Chem. B* **2001**, *105*, 3908–3916.
(14) Kershen, K.; Celio, H.; Lee, I.; White, J. M. *Langmuir* **2001**, *17*, 323–328.
(15) Tamura, M.; Kochi, J. K. *Bull. Chem. Soc. Jpn.* **1972**, *45*, 1120–1127.
(16) Filinchuk, Y.; Chernyshov, D.; Nevidomskyy, A.; Dmitriev, V. *Angew. Chem., Int. Ed.* **2008**, *47*, 529–532.
(17) Filinchuk, Y.; Talyzin, A. V.; Chernyshov, D.; Dmitriev, V. *Phys. Rev. B* **2007**, *76*, 092104−1–092104−4.
(18) Černý, R.; Filinchuk, Y.; Hagemann, H.; Yvon, K. *Angew. Chem., Int. Ed.* **2007**, *46*, 5765–5767.
(19) Birker, P. J. M. W. L.; Reedijk, J.; Verschoor, G. C. *Inorg. Chem.* **1981**, *20*, 2877–2882.

 Published on Web 12/21/2009

Ag(I) to form various high nuclearity complexes and polymers with chalcogen donor ligands is well-known.[20] Our group has reported the formation of octanuclear silver clusters which can entrap a selenide, a bromide, or a chloride anion inside an Ag_8 cubic cage supported by diselenophosphate ligands (abbreviated as dsep).[21−23] In addition, our group has also reported undecanuclear silver clusters in which a selenide was entrapped inside the pentacapped trigonal prismatic silver cage.[24] Besides, Matsumoto et al. reported a "S" inside the Ag_8 cube supported by dithiophosphates.[25] However, there is no precedence of any silver cluster core adopting tetracapped-tetrahedral geometry, as only recently our group made possible to report few Cu_8 clusters with a tetracapped-tetrahedral core while recognizing the smallest closed-shell anion, hydride, inside the copper cage, and these are the only examples of octanuclear homometallic clusters displaying in such a geometry.[26,27]Herein, we present the first stable structures of silver(I)-hydride clusters supported by dialkyl diselenophosphate ligands in which the presence of hydride is unequivocally authenticated by both ^{1}H and ^{109}Ag NMR spectroscopies.

Results and Discussion

The reaction of $Ag(CH_3CN)_4PF_6$ with $NH_4Se_2P(OR)_2$ in an 8:6 ratio for 1 h in THF followed by the addition of one equivalent of $NaBH_4$ at −20 °C produced $[Ag_8(H)\{Se_2P(OR)_2\}_6](PF_6)$ [R = ^{i}Pr, **1**; Et, **2**] in good yield. A similar reaction carried out with the use of $NaBD_4$ instead of $NaBH_4$ resulted in $[Ag_8(D)\{Se_2P(OR)_2\}_6](PF_6)$ [R = ^{i}Pr, $\mathbf{1_D}$; Et, $\mathbf{2_D}$]. Good quality single crystals suitable for X-ray diffraction studies were grown from acetone.

Crystallography. The structure analysis of cluster cation **1** reveals that all of the eight silver atoms are disordered in two positions, each of them in 50% occupancy to form two cubes with one inside the other (Scheme 1), but only four of them in each cube are actually fully occupied along with six dsep ligands and the PF_6^-. In addition, a hydride is located in the crystallographic center of inversion. On the basis of both ^{31}P and ^{77}Se NMR results (vide infra) which require the coexistence of C_2 and C_3 rotational axes in order to keep all six dsep ligands equivalent magnetically, a hydride-centered tetracapped-tetrahedral silver framework is modeled (Figure 1a). A similar disordered metallic core was observed in the analogous copper complexes.[26,27] Four silver atoms Ag1, Ag2A, Ag3A, and Ag4 (abbreviated as Ag_v), comprised the inner tetrahedron, are

Scheme 1

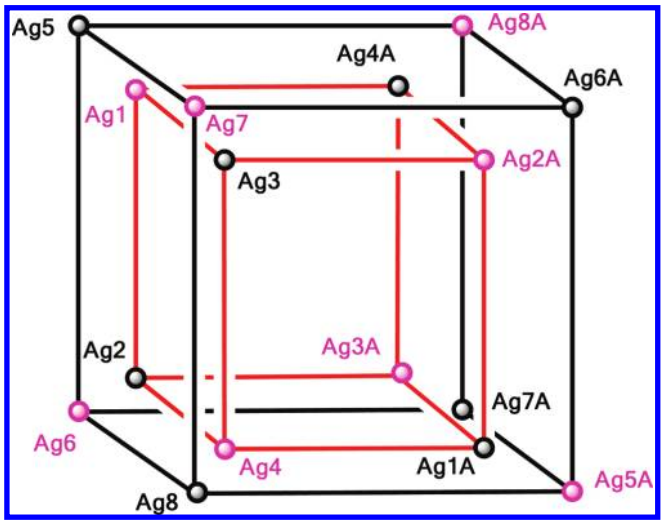

directly connected to the interstitial hydride and each triangular face of this tetrahedron is capped by the capping Ag atoms namely Ag5A, Ag6, Ag7, and Ag8A (abbreviated as Ag_{cap}). The edge of the inner Ag_4 tetrahedron ranges from 3.084 to 3.235 Å, and the distances between the capping Ag atom and the vertex of the tetrahedron are in the range of 2.989−3.141 Å, which are significantly shorter than the sum of the van der Waals radii for silver (3.40 Å).[28] Distances between the interstitial hydride and four, directly linked silver atoms are in the range of 1.872(1)−2.031(2) Å. These are slightly longer than 1.831(5) Å identified in $[(PEt_3)_2(C_6Cl_5)Pt(\mu\text{-}H)Ag(H_2O)]^+$,[10] and the sum of the covalent radii, 1.76(5) Å.[29] The tetracapped tetrahedron is further surrounded by twelve Se atoms from six bridging dsep ligands in a nearly icosahedral skeleton. Thus, **1** represents *the first example of a tetracapped tetrahedral silver framework inscribed in a Se_{12} icosahedral cage*. Six dsep ligands, each retaining a trametallic, tetraconnective pattern (μ_2, μ_2) are located on the top of Ag_4 butterflies where hinge positions are edges of the tetrahedron and wingtips are capping Ag atoms (Figure 1b). The dihedral angles of the Ag_4 butterfly range from 148−152°. Two kinds of Se−Ag distances are observed with the shorter one being connected to the capping Ag atoms (Ag_{cap}). While the Ag_{cap}−Se lengths, 2.449(1)−2.554(2) Å, are normal,[30] the Ag_v-Se distances, 2.730(2)−2.832(2)Å, are relatively long. The Se···Se "bite" distances are averaged at 3.756 Å. Both P−O [1.519(9)−1.582(6) Å] and P−Se [2.158(3)−2.169(2) Å] bond lengths are within the reported values.[30] Overall a C_3 rotational axis passes through the vertex of the inner tetrahedron, the central hydride, and a capping Ag atom opposite to the vertex. The three C_2 axes, each being colinear with a line passing through two opposite P atoms and the central hydride, constitute an idealized T symmetry for the cluster cation **1**.

(20) Degroot, M. W.; Corrigan, J. F. High Nuclearity Clusters: Metal−Chalcogenide Polynuclear Complexes. In *Comprehensive Coordination Chemistry II*; Fujita, M., Powell, A., Creutz, C., Eds.; Elsevier: New York, 2005; Vol. *7*, pp 57−123.
(21) Liu, C. W.; Shang, I.-J.; Wang, J.-C.; Keng, T.-C. *Chem. Commun.* **1999**, 995–996.
(22) Liu, C. W.; Hung, C.-M.; Haia, H.-C.; Liaw, B.-J.; Liou, L.-S.; Tsai, Y.-F.; Wang, J.-C. *Chem. Commun.* **2003**, 976–977.
(23) Liu, C. W.; Haia, H.-C.; Hung, C.-M.; Santra, B. K.; Liaw, B.-J.; Lin, Z.; Wang, J.-C. *Inorg. Chem.* **2004**, *43*, 4464–4470.
(24) Liu, C. W.; Shang, I.-J.; Fu, R.-J.; Liaw, B.-J.; Wang, J.-C.; Chang, I.-J. *Inorg. Chem.* **2006**, *45*, 2335–2340.
(25) Matsumoto, K.; Tanaka, R.; Shimomura, R.; Nakao, Y. *Inorg. Chim. Acta* **2000**, *304*, 293–296.
(26) Liao, P.-K.; Sarkar, B.; Chang, H.-W.; Wang, J.-C.; Liu, C. W. *Inorg. Chem.* **2009**, *48*, 4089–4097.
(27) Liu, C. W.; Sarkar, B.; Huang, Y.-J.; Liao, P.-K.; Wang, J.-C.; Saillard, J.-Y.; Kahlal, S. *J. Am. Chem. Soc.* **2009**, *131*, 11222–11233.
(28) Bondi, A. *J. Phys. Chem.* **1964**, *68*, 441–451.
(29) Cordero, B.; Gomez, V.; Platero-Prats, A. E.; Reves, M.; Echeverria, J.; Cremades, E.; Barragan, F.; Alvarez, S. *Dalton. Trans.* **2008**, 2832–2838.
(30) Lobana, T. S.; Wang, J.-C.; Liu, C. W. *Coord. Chem. Rev.* **2007**, *251*, 91–110.

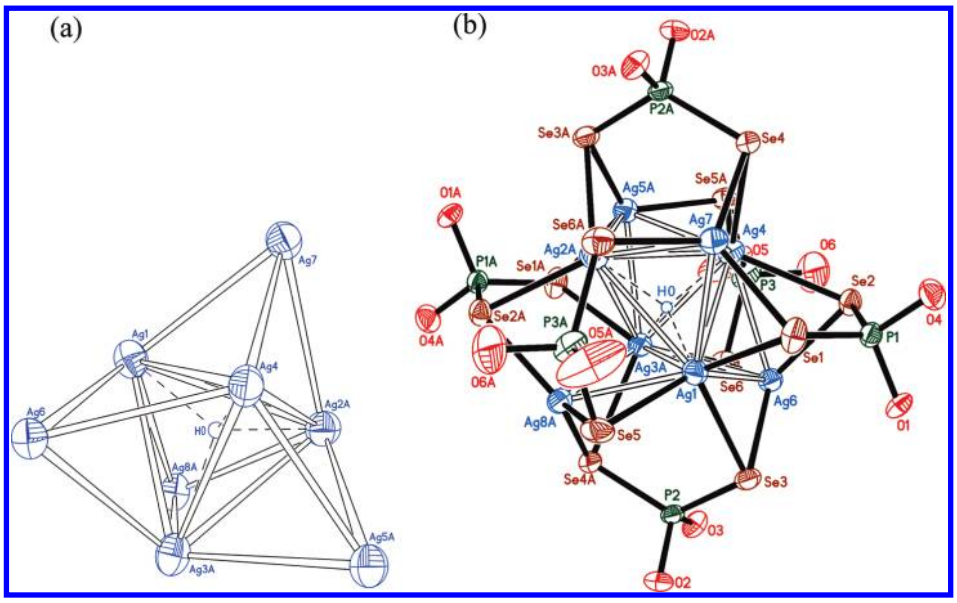

Figure 1. (a) Central unit $[Ag_8H]$ in **1**. (b) Molecular structure of $[Ag_4(\mu_4\text{-}H)(\mu_3\text{-}Ag)_4\{Se_2P(O^iPr)_2\}_6]^+$ (50% thermal ellipsoid) with isopropyl groups omitted for clarity.

In contrary to the two, disordered silver frameworks of **1** in equal probability, the silver skeleton of ethyl derivative **2**, which crystallized in the $R\bar{3}c$ space group, is also disordered in two orientations, but the major component in 75% occupancy. Both Ag1 and Ag3 with their symmetry generated atoms from the inner tetrahedron which is connected directly to the hydride whereas Ag2, and Ag4 atoms constitute the Ag_{cap} (Figure 2). Although Ag_v-Ag_v distances in the range 3.069(2)−3.189(3) Å are slightly shorter than Ag_v-Ag_{cap} distances (3.041(2)−3.243(2) Å), yet all of them remain below the sum of van der Waals radii for silver (3.40 Å),[28] indicative of argentophillic interaction.[31] The average Ag−H distances in **2** (1.927 Å) are however slightly shorter than that in **1** (1.937 Å). Relevant bond lengths are listed in Table 1.

NMR. A singlet flanked with a pair of Se satellites (80.6 ppm, J_{PSe} = 646 Hz) in the $^{31}P\{^1H\}$ NMR spectrum and a doublet (−0.2 ppm, J_{SeP} = 648 Hz) in the $^{77}Se\{^1H\}$ NMR spectrum are observed for **1**. Thus all the P and Se atoms in **1** are equivalent in solution. The ^1H NMR spectrum of **1** displays a set of chemical shifts corresponding to the isopropyl group, and an apparent nonet resonance centered at 3.14 ppm that integrates to 1H relative to twelve methine protons of the six isopropyl groups (Figure 3a). Thus, this peak could correspond to the hydride resonance. It does not display obvious line shape change upon the decrease in temperature up to 193 K, but shifted ∼0.5 ppm upfield at −80 °C presumably due to the consequence of metallic core shrinkage (Figure S1 of the Supporting Information). The coupling constant (J_{HAg} = 33.2 Hz) is comparable to the number observed in mixed Ru−H−Ag clusters,[4] but much smaller than those observed in other heterometallic silver hydride complexes.[5−10] This nonet peak in which the separate $^1H-^{109}Ag$ and $^1H-^{107}Ag$ couplings are not resolved becomes a seventeen-line band ($J_{1H\text{-}107Ag}$ = 30.8 Hz)

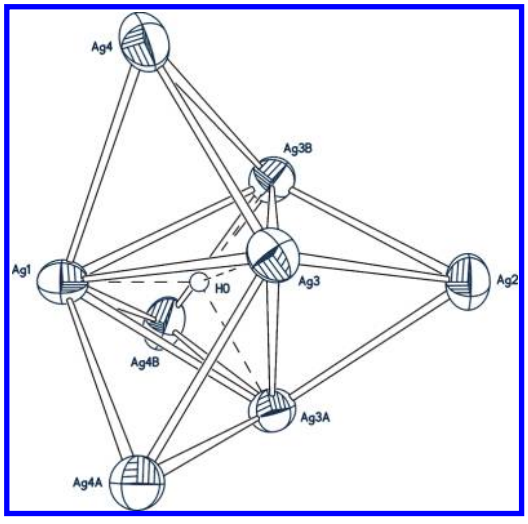

Figure 2. Central unit $[Ag_8H]$ in **2**.

(Figure 3b) after decoupling of the ^{109}Ag nuclei (I = 1/2, 48.18%). The integration ratio of the nonet resonance observed to be 2.3:7.2:27.8:57.8:75.5:58.0:28.5:8.0:2.5, in the ^1H NMR spectrum after deconvolution by Lorentzian shape, is close to the theoretical ratio of 1:8:28:56:70:56:28:8:1, a proton coupled to eight silver nuclei (Figure S2). The deviation of the two outermost peaks is due to the overlapping with unknown peaks. Similarly, the integration ratio for the central, 11 peaks of the 17-line splitting pattern in the $^1H\{^{109}Ag\}$ spectrum is also close to the theoretical ratio (Figure S3). The intensities of the two outermost peaks indicated by asterisks in Figure 3b are very weak and overlapped with some noises. The spectroscopic data clearly suggest that the proton is coupled to eight equivalent ^{107}Ag nuclei.

The hydride assignment was also confirmed with the corresponding deuteride complex $\mathbf{1_D}$. Its spectroscopic data (^{31}P and ^{77}Se NMR) are almost similar to **1** (see the Experimental Section). Most importantly, a multiplet at 3.14 ppm is revealed in the ^2H NMR spectrum. Furthermore, both **2**

(31) Pyykkö, P. *Chem. Rev.* **1997**, *97*, 597–636.

Table 1. Selected Bond Lengths (Å) and Bond Angles (deg) with esd's in the Parentheses

	1	**2**
Ag−H	1.8723(13), 1.8912(15), 1.9533(17), 2.0306(17)	1.74(16), 1.99(7)
Ag_v—Ag_v [a]	3.0841(18), 3.102(2), 3.151(2), 3.184(2), 3.223(2), 3.235(4)	3.069(2), 3.189(3)
Ag_v—Ag_{cap} [b]	2.9888(17), 3.000(2), 3.001(2), 3.0055(19), 3.0059(19), 3.0188(19), 3.0238(18), 3.0280(19), 3.029(2), 3.073(2), 3.0970(19), 3.1411(19)	3.041(2), 3.0393(19), 3.110(2), 3.2433(18)
Ag_v—Se	2.7523(16), 2.7995(15), 2.8045(17), 2.7296(16), 2.7382(16), 2.7911(17), 2.7607(17), 2.7625(16) 2.7787(15), 2.7538(16), 2.7918(15), 2.8315(17)	2.7096(16), 2.7170(16), 2.7740(18), 2.7971(19)
Ag_{cap}—Se	2.4589(16), 2.4680(17), 2.5517(16), 2.5026(17), 2.5462(15), 2.5538(15), 2.4760(16), 2.5066(18), 2.5117(16), 2.4490(17), 2.5181(18), 2.5212(16)	2.5432(19), 2.5530(18), 2.627(2), 2.5630(16)
Se···Se (bite)	3.765(4), 3.768(5), 3.774(4),	3.739(2), 3.779(2)
Se−P	2.158(3), 2.159(2), 2.161(3), 2.166(2), 2.167(2), 2.169(2),	2.145(5), 2.149(3), 2.161(4), 2.171(3)
Se−P−Se	120.59(10), 121.44(9), 121.50(10)	122.03(14), 120.55(17)
O−P−O	102.8(3), 103.9(8), 108.3(3)	108.3(5), 95.5(14)
dihedral angles of Ag_4 butterfly	148, 150, 153	145, 152

[a] Ag_v = Ag atoms at the vertex of the tetrahedron. [b] Ag_{cap} = Ag atoms capped to the tetrahedron face.

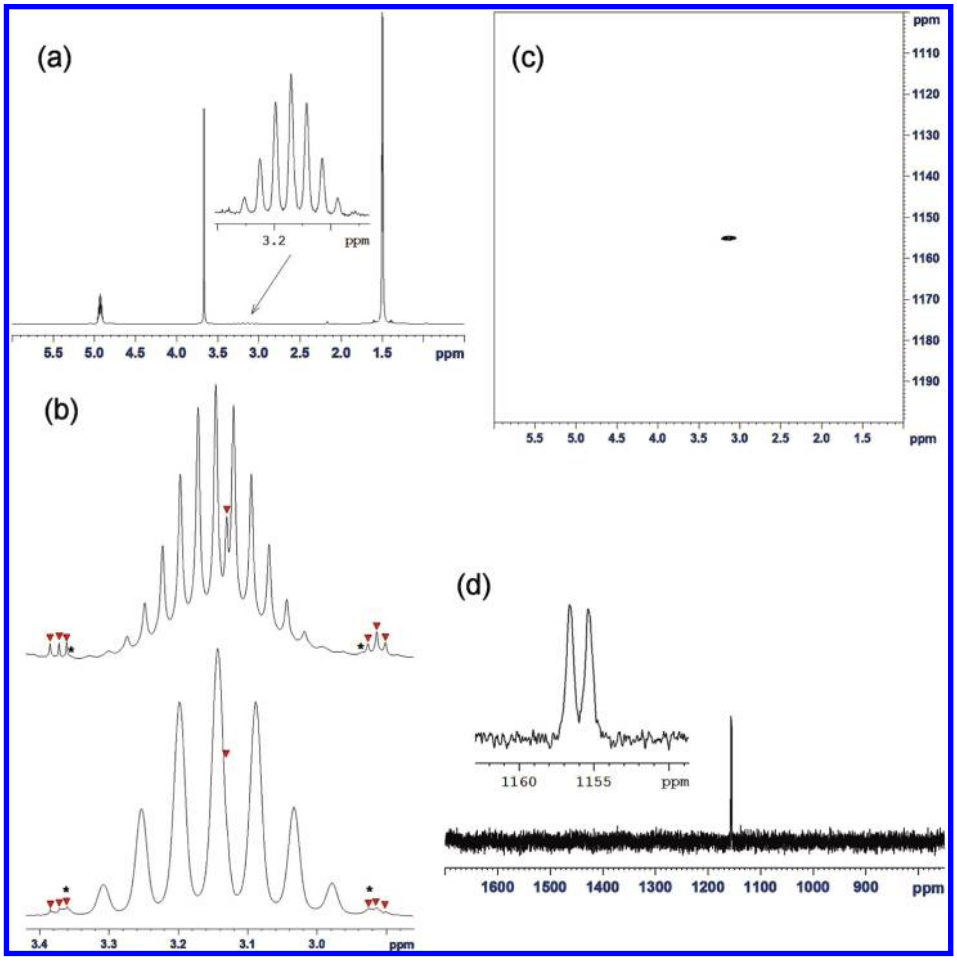

Figure 3. (a) ^{1}H NMR of **1** with the magnified, hydride resonance shown in the inset. The δ at 3.7 ppm is the H_2O resonance. (b) Hydride resonance of ^{1}H NMR of **1** (bottom); hydride resonance of ^{1}H{^{109}Ag} NMR of **1** (top). Whereas the asterisks indicate the two outermost peaks, uncharacterized peaks are depicted by the red triangle. (c) ^{1}H−^{109}Ag HMQC. (d) ^{109}Ag NMR of **1** with the magnified spectrum shown in the inset.

and $\mathbf{2_D}$ exhibit a similar singlet in ^{31}P NMR spectra in addition to a doublet in the ^{77}Se NMR spectra. The ^{1}H NMR spectrum of **2** showed the resonances for the ethyl protons as well as a multiplet at 3.04 ppm for the hydride. Although the coupling pattern is not well resolved as identified in **1**, yet the coupling constant (J_{HAg} = 30 Hz) is comparable with **1** and the integration ratio of this proton with respect to methylene protons of the ethyl group is approximately 1:24. $\mathbf{2_D}$ even showed the deuteride peak at 3.23 ppm as a multiplet in ^{2}H NMR. It should be noted here that although the isostructural copper complex [Cu_8(μ_4−H){$Se_2P(O^iPr)_2$}$_6$](PF_6) exhibited a broad singlet at −0.58 for the hydride in ^{1}H NMR spectrum,[27] a positive chemical shift for hydride was indeed reported in [($C_5Me_4SiMe_3$)YH_2]$_4$(THF),[32] the first four-coordinate hydrogen atom in a tetrahedral cavity. This is not surprising as the

(32) Yousufuddin, M.; Gutmann, M. J.; Baldamus, J.; Tardif, O.; Hou, Z.; Mason, S. A.; Mclntyre, G. J.; Bau, R. *J. Am. Chem. Soc.* **2008**, *130*, 3888–3891.

Scheme 2

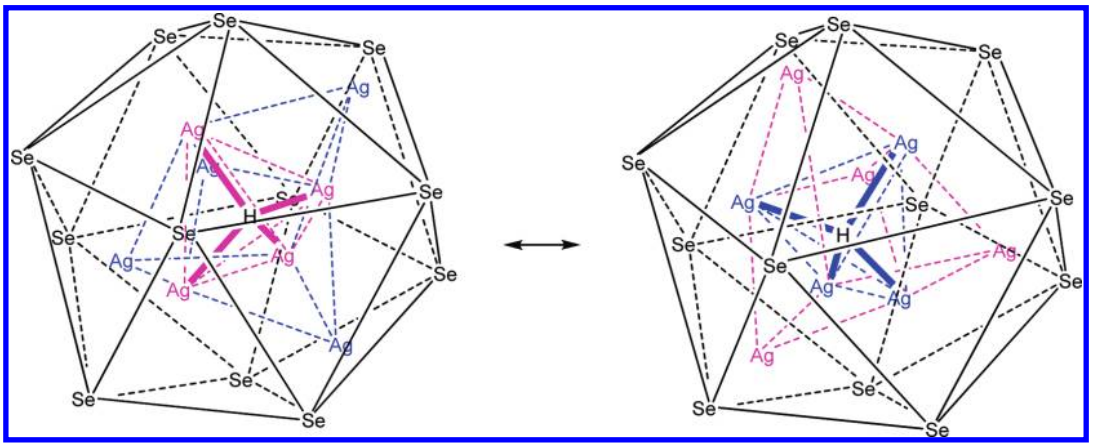

chemical shifts of interstitial hydride are known to vary over a range of +15.5 to −26.8 ppm, and it has been suggested that hydrides that are located in the center of a regular octahedron display the lowest-field chemical shifts while those more asymmetrically oriented have high-field chemical shifts.[33]

Further evidence that the hydride is connected to the Ag atoms in **1** is obtained from $^{1}H-^{109}Ag$ HMQC (heteronuclear multiple-quantum correlation) experiment (Figure 3c) which provides the resonance of silver nuclei and matches well with a doublet peak obtained in the single pulse sequence ^{109}Ag NMR spectrum (δ 1155.2 ppm, $J_{1H-109Ag} = 35.0$ Hz) (Figure 3d). This chemical shift is also close to the silver resonance revealed in $[Ag\{P(OEt)_3\}_3](NO_3)$.[34] Similarly, a doublet was observed for **2** whereas the corresponding deuteride species $\mathbf{1_D}$ and $\mathbf{2_D}$ revealed an unresolved broad singlet centered at 1155.2 and 1148.4 ppm, respectively, in their single pulse ^{109}Ag NMR spectra. Thus the ^{109}Ag NMR spectrum strengthens the fact that all the eight silver nuclei of **1** and **2** are equivalent in solution.

Besides, the exact one mass unit difference for the cationic fragment of $[Ag_8(X)\{Se_2P(OEt)_2\}_6]^+$ (X = H or D) is observed in the positive ESI-MS spectra of both **2** and $\mathbf{2_D}$ (m/z 2536.1 and 2537.1). A similar −1 amu shift for $[Cu_8(X)\{Se_2P(O^iPr)_2\}_6]^+$ (X = H or D) was observed in addition to the exact 1 amu difference between hydride and deuteride species.[27]

In sharp contrast to the crystallographic studies that reveal the hydride being connected only to four Ag out of eight silver atoms inscribed in a Se_{12} icosahedron in tetracapped-tetrahedral geometry, the nine-line splitting pattern for the hydride resonance in ^{1}H NMR of **1** as well as a doublet peak observed in the ^{109}Ag NMR clearly suggests that it is due to the coupling of the hydrogen with eight chemically equivalent silver nuclei, not just four. It is unlikely that the tetracapped tetrahedral Ag_8 core undergoes a structural change in solution to form a regular cube of T_h symmetry, which is energetically unfavorable as suggested by a DFT calculation (vide infra). Thus, we

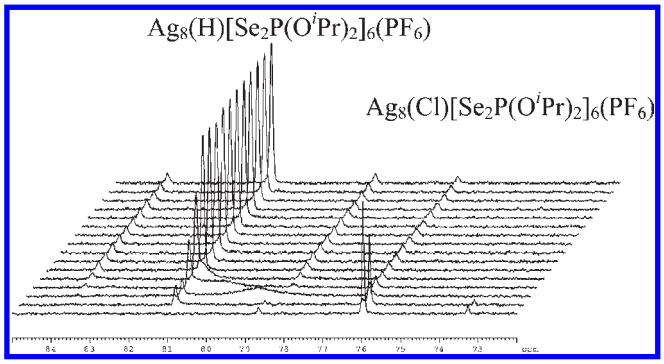

Figure 4. Progress of the reaction from $[Ag_8(Cl)\{Se_2P(O^iPr)_2\}_6]^+$ to $[Ag_8(H)\{Se_2P(O^iPr)_2\}_6]^+$ in the presence of $NaBH_4$ monitored by ^{31}P NMR spectroscopy.

propose that the exchange of silver atoms between capping and vertex positions as shown in the Scheme 2 is so fast that all eight silver nuclei are equivalent on the NMR timescale. This is reminiscent of the stability of the Ag(I) cubic cluster inscribed in a E_{12} (E = S, Se) icosahedral cage which, in general, is due to the chelating "pinch" effect of the dichalcophosphate ligands.[24] Hence a range of "energetically reasonable" Ag···Ag distances and some degree of metal framework distortion apparently exists with these ligands. However, the aforementioned exchange of metallic core does not alter the structure or property of the complexes as we observed that the powder X-ray diffraction (XRD) patterns before and after the NMR experiment are virtually the same (Figure S4, Supporting Information).

Furthermore, the facts that encapsulated hydride in both **1** and **2** cannot be exchanged with the deuteride and even the acidification of both **1** and **2** does not break the complexes to produce H_2 which is confirmed by NMR experiments suggest the high stability of the complexes.

Similar to the recent report of hydride-centered octanuclear copper clusters which can be generated from the corresponding chloride-centered Cu_8^I clusters surrounded by six dithiophosphate ligands,[26] **1** and **2** can also be isolated from the reaction of $[Ag_8(Cl)\{SeP(OR)_2\}_6]^+$ with $NaBH_4$ within 2 min which can be monitored by ^{31}P NMR spectroscopy (Figure 4). The speed of this reaction suggests Cl-centered compounds acted as a hydride sponge to produce the title compounds.

(33) Eguchi, T.; Heaton, B. T. *J. Chem. Soc., Dalton Trans.* **1999**, 3523–3530.
(34) Colquhoun, I. J.; McFarlane, W. *J. Chem. Soc., Chem. Commun.* **1980**, 145–147.

Table 2. Relevant Computed Results on the $[Ag_8(Se_2PH_2)_6]^{2+}$ and $[Ag_8(H)(Se_2PH_2)_6]^{+}$ Models

	$[Ag_8(Se_2PH_2)_6]^{2+}$	$[Ag_8(H)(Se_2PH_2)_6]^{+}$	
symmetry	T_h	T_h	T
relative energy/eV		0.67	0.00
HOMO−LUMO gap/eV	2.71	2.89	3.01
Ag−Ag (cube edge)/Å	3.621	2.995	3.145[a]
Ag−Ag (core tetrahedron edge)/Å		4.236[b]	3.239
Ag−H/Å		2.594	1.984
			3.190
Ag−Se/Å	2.663	2.726	2.808
			2.696
Se···Se/Å	3.942	3.902	3.883
relative energy of the $[Ag_8(Se_2PH_2)_6]^{2+}$ fragment/eV[c]	0.00	0.68	0.83
bonding energy between the $[Ag_8(Se_2PH_2)_6]^{2+}$ and H^- fragments/eV[c]		10.51	11.32
natural orbital population analysis of the encapsulated hydride		$1s^{1.65}$	$1s^{1.63}$

[a] Distorted cube. [b] Square face diagonal. [c] See Computational Details.

Theoretical Investigation. We have also addressed the question of the existence or lack of a tetrahedral distortion in the title octanuclear silver clusters via a density functional theory (DFT) investigation on the simplified model $[Ag_8(H)(Se_2PH_2)_6]^{+}$ and on its parent empty cluster $[Ag_8(Se_2PH_2)_6]^{2+}$. Relevant results are given in Table 2. Whereas the equilibrium structure of the hypothetical $[Ag_8(Se_2PH_2)_6]^{2+}$ cage was found to adopt a regular cubic arrangement of T_h symmetry, the tetrahedrally distorted T structure was found to be the energy minimized one for the hydride model $[Ag_8(H)(Se_2PH_2)_6]^{+}$. Clearly, the Ag_8 framework of this structure should be described as a tetracapped-tetrahedron, with tetrahedron edges of 3.239 Å and capping distances of 3.145 Å, and the encapsulated hydride is bonded to the four Ag atoms forming the central tetrahedron (Ag−H = 1.984 Å). Geometry optimization of $[Ag_8(H)(Se_2PH_2)_6]^{+}$ under the T_h symmetry constraint, leads to a structure which is 0.67 eV (15 kcal/mol) less stable than the T structure, a value far from being negligible. Moreover, with several computed imaginary vibrational frequencies (largest value = 244i, for a vibration of t_u symmetry), the T_h structure is not an energy minimum or a transition state. The tetrahedral contraction afforded by the $[Ag_8(Se_2PH_2)_6]^{2+}$ cage upon the formal incorporation of a hydride in its center increases the bonding energy between these two fragments to a greater extent than it destabilizes the empty cubic cage (Table 2). With a hydride donation to the cage of 0.37 electron, the bonding between these fragments is largely covalent. These results are very similar to those computed for the related $[Cu_8(H)(E_2PH_2)_6]^{+}$ (E = Se, S) series.[27] Therefore, the DFT calculations on the $[Ag_8(H)(Se_2PH_2)_6]^{+}$ model predict a tetracapped-tetrahedral geometry in the gas phase which is in an excellent agreement with the crystal structures of **1** and **2**. On the other hand, the proton and silver NMR behaviors of the latter clusters seem to be consistent with the existence of eight equivalent silver nuclei. Thus, the chemical shift of the hydride in $[Ag_8(H)(Se_2PH_2)_6]^{+}$ has been computed by using the GIAO method (see Computational Details). The computed chemical shift for the equilibrium T geometry (4.5 ppm) is ∼1.5 ppm larger than the experimental one. This is a rather good agreement owing to the level of theory and modelization. On the other hand, the computed value for the unstable T_h structure (9.2 ppm) is quite far off the experimental data. Furthermore, a similar, small positive discrepancy of the hydride chemical shift computed at the same level of theory on the equilibrium T geometry was found between the copper model $[Cu_8(H)(Se_2PH_2)_6]^{+}$ (0.7 ppm) and the experimental value (−0.5 ppm).[27] These results strongly suggest that the structures of **1** and **2** in solution is not the cubic but rather the tetracapped-tetrahedral type and that a fast equilibrium, which interchanges the relative positions of the two types of silver atoms, is taking place. This equilibrium should involve a transition state (possibly a reaction intermediate) of lower symmetry and lower energy than the cubic T_h structure. The exploration of this low-energy mechanism by DFT calculations is currently underway.

In conclusion, we have demonstrated the synthesis and structural characterization of the first stable Ag(I)-hydride species in which hydride is solely coordinated to Ag(I). The entrapment of the smallest closed-shell anion, hydride, induces the tetrahedral distortion of the Ag_8 core geometry, which is normally cubic in order to accommodate a larger closed-shell anion, to adopt the tetracapped tetrahedron. This uncommon geometry is also confirmed by a DFT calculation on a model compound which suggested that the Ag_8H cubic core of T_h symmetry may not be formed as it is energetically highly unfavorable. Furthermore, solution NMR (^1H and ^{109}Ag) data clearly suggest that a fast equilibrium which interchanges the role of capping and vertex silver atoms in solution must occur. Thus, the implication of this work may lead to better control of metal cluster geometry upon entrapment of small anions in general.

Experimental Section

All chemicals were purchased from commercial sources, and used as received. Solvents were purified following standard protocols.[35] All the reactions were performed in oven-dried Schlenk glassware by using standard inert-atmosphere techniques. $NH_4Se_2P(O^iPr)_2$ and $NH_4Se_2P(OEt)_2$[36] were prepared according to the reported methods. All the reactions were carried out under N_2 atmosphere by using standard Schlenk techniques. The elemental analyses were done using a Perkin-Elmer 2400 CHN analyzer. ^1H and ^{109}Ag NMR

(35) Perrin, D. D.; Armarego, W. L. F.; Perrin, D. R. *Purification of Laboratory Chemicals*, 2nd ed.; Pergamon Press: Oxford, 1980.
(36) Liu, C. W.; Shang, I.-J.; Hung, C.-M.; Wang, J.-C.; Keng, T.-C. *J. Chem. Soc., Dalton Trans.* **2002**, 1974–1979.

spectra of **1** were recorded on a Bruker Avance III 600 NMR which operates at 600 MHz for ^{1}H and 27.9 MHz for ^{109}Ag nuclei. All other NMR spectra were recorded on Bruker Advance DPX300 FT-NMR spectrometers which operate at 300 MHz for ^{1}H, 121.5 MHz for ^{31}P, 57.2 MHz for ^{77}Se, and 46.1 MHz for ^{2}H nuclei. The ^{31}P{^{1}H}, and ^{77}Se{^{1}H} NMR are referenced externally against 85% H_3PO_4 (δ = 0 ppm) and PhSeSePh (δ = 463 ppm), respectively. The chemical shift (δ) and coupling constant (J) are reported in parts per million and hertz, respectively. The NMR spectra were recorded at ambient temperature if not mentioned. Melting points were measured by using Fargo MP-2D melting point apparatus. ESI-Mass spectra were recorded on a Fison Quattro Bio-Q (Fisons Instruments, VG Biotech, UK).

Safety Note. *Selenium and its derivatives are toxic! These materials should be handled with great caution.*

Synthesis. **$[Ag_8(H)\{Se_2P(O^iPr)_2\}_6](PF_6)$, 1.** A solution of $NH_4[Se_2P(O^iPr)_2]$ (0.2 g, 0.615 mmol), $Ag(CH_3CN)_4PF_6$ (0.342 g, 0.820 mmol), and $NaBH_4$ (0.0039 g, 0.103 mmol) in 20 mL of THF was stirred at −20 °C for 1 h under nitrogen. It was then filtered to get rid of any solid, and the filtrate was evaporated to dryness to get a brown solid. It was washed with deionized water followed by diethyl ether and then dried under vacuum to obtain $[Ag_8(\mu_4\text{-}H)\{Se_2P(O^iPr)_2\}_6](PF_6)$ as a brown powder. Yield: 0.169 g (58%). Mp: 152 °C. Anal calcd for $Ag_8H_{85}C_{36}O_{12}P_7F_6Se_{12}$: C 15.16; H 3.00. Found: C 15.00; H 3.22%. ^{1}H NMR (600 MHz, acetone-d_6): 1.41 (d, $^{3}J_{HH}$ = 5.8 Hz, 72H, CH_3), 3.14 (nonet, J_{HAg} = 33.2 Hz, 1H), 4.80(m, 12H, CH). ^{31}P NMR (acetone-d_6): 80.6 ($^{1}J_{PSe}$ = 646 Hz). ^{77}Se NMR (acetone-d_6): −0.2 (d, $^{1}J_{PSe}$ = 648 Hz); ^{109}Ag NMR (acetone-d_6): 1155.2 (d, J_{AgH} = 35.0 Hz).

$[Ag_8(D)\{Se_2P(O^iPr)_2\}_6](PF_6)$, 1_D. It can be obtained via a similar procedure as described for **1** except $NaBD_4$ was used instead of $NaBH_4$. Yield: 0.180 g (62%). Mp: 155 °C (decomp). Anal calcd for $Ag_8H_{84}C_{36}O_{12}P_7F_6Se_{12}D_1\cdot 2H_2O$: C 14.97; H 3.14. Found: C 14.68; H 3.20%. ^{1}H NMR (300 MHz, acetone-d_6): 1.41 (d, $^{3}J_{HH}$ = 5.8 Hz, 72H, CH_3), 4.80 (m, 12H, CH). ^{2}H NMR (46.1 MHz, acetone-d_6): 3.23 (m, $J_{D\text{-}Ag}$ = 5 Hz, D). ^{31}P NMR (acetone-d_6): 80.4 (J_{PSe} = 647 Hz). ^{77}Se NMR (acetone-d_6): 0.7 (d, J_{PSe} = 647 Hz). ^{109}Ag NMR (acetone-d_6): 1155.2 (bs).

$[Ag_8(H)\{Se_2P(OEt)_2\}_6](PF_6)$, 2. It was synthesized in a similar manner as described for compound **1**, however $NH_4[Se_2P(OEt)_2]$ was used instead of $NH_4[Se_2P(O^iPr)_2]$. Yield: 0.166 g (55%). Mp: 148 °C. Anal calcd for $Ag_8H_{61}C_{24}O_{12}P_7F_6Se_{12}\cdot 0.5(C_2H_5)_2O$: C 11.48; H 2.45. Found: C 11.54; H 2.70%. ^{1}H NMR (acetone-d_6): 1.49 (t, $^{3}J_{HH}$ = 7.1 Hz, 36H, CH_3), 3.04 (m, J_{HAg} = 30.0 Hz, 1H), 4.23 (m, 24H, CH_2). ^{31}P NMR (acetone-d_6): 86.7 ($^{1}J_{PSe}$ = 654 Hz). ^{77}Se NMR (acetone-d_6): −24.0 (d, $^{1}J_{PSe}$ = 655 Hz). ^{109}Ag NMR (acetone-d_6): 1148.4 (d, J_{AgH} = 30.0 Hz). Positive ion ESI-MS (m/z)(cal): 2536.1 (2536.5) $[Ag_8(H)\{Se_2P(OEt)_2\}_6]^+$.

$[Ag_8(D)\{Se_2P(OEt)_2\}_6](PF_6)$, 2_D. It was synthesized in a similar manner as described for compound **1**; however, $NH_4[Se_2P(OEt)_2]$ was used instead of $NH_4[Se_2P(O^iPr)_2]$ and $NaBD_4$ was used instead of $NaBH_4$. Yield: 0.174 g (58%). Mp: 148 °C (decomp). Anal. calcd for $Ag_8H_{60}C_{24}O_{12}P_7F_6Se_{12}D_1$: C 10.74; H 2.33. Found: C 11.01; H 2.43%. ^{1}H NMR (acetone-d_6): 1.49 (t, $^{3}J_{HH}$ = 7.1 Hz, 36H, CH_3), 4.23 (m, 24H, CH_2). ^{2}H NMR (acetone-d_6): 3.23 (m, D). ^{31}P NMR (acetone-d_6): 86.7 ($^{1}J_{PSe}$ = 655 Hz). ^{77}Se NMR (acetone-d_6): −23.5 (d, $^{1}J_{PSe}$ = 656 Hz). ^{109}Ag NMR (acetone-d_6): 1148.4 (bs). Positive ion ESI-MS (m/z)(cal): 2537.1 (2538.5) $[Ag_8(D)\{Se_2P(OEt)_2\}_6]^+$.

X-ray Crystallography. Crystals were mounted on the tips of glass fibers with epoxy resin. Data were collected on a Bruker APEXII CCD diffractometer using graphite monochromated Mo Kα radiation (λ = 0.71073 Å). Absorption corrections for the area detector were performed with the program SADABS.[37]

Table 3. Selected Crystallographic Data for Compounds **1** and **2**

	1	**2**
formula	$C_{36}H_{85}Ag_8F_6O_{12}P_7Se_{12}$	$C_{24}H_{61}Ag_8F_6O_{12}P_7Se_{12}$
F_w	2851.31	2683.00
space group	$P\bar{1}$	$R\bar{3}c$
a, Å	13.048(2)	17.8467(9)
b, Å	13.1199(12)	17.8467(9)
c, Å	13.8959(13)	74.722(4)
α, deg	116.883(2)	90
β, deg	99.052(2)	90
γ, deg	95.746(2)	120
V, Å^3	2055.4(5)	20610.8(18)
Z	1	12
ρ_{calcd}, g cm^{-3}	2.304	2.594
μ, mm^{-1}	7.368	8.808
T, K	296(2)	293(2)
reflections collected	21308	19353
independent reflections	10080 [R_{int} = 0.0489]	4030 [R_{int} = 0.0449]
$R1^a$, $wR2^b$ [$I > 2\sigma(I)$]	0.0565, 0.1441	0.0631, 0.1870
$R1$, $wR2$ (all data)	0.1067, 0.1793	0.0917, 0.2057
goodness of fit	1.025	1.087
largest diff peak and hole, e/Å^3	1.185 and −1.255	1.352 and −1.530

^{a} $R1 = \sum||F_o|-|F_c||/\sum|F_o|$. ^{b} $wR2 = \{\sum[w(F_o^2-F_c^2)^2]/\sum[w(F_o^2)^2]\}^{1/2}$.

Structures were solved by direct methods and were refined against the least-squares methods on F^2 with the SHELXL-97 package,[38] incorporated in SHELXTL/PC V5.10.[39] Pertinent crystallographic data are listed in Table 3.

Computational Details. DFT calculations were carried out using the Gaussian 03 package,[40] employing BP86 functionals,[41] and using the general triple-ξ polarized basis set, namely the Def2-TZVP set from the EMSL Basis Set Exchange Library.[42] All stationary points were fully characterized as true mimina via analytical frequency calculations. The geometries obtained from DFT calculations were used to perform natural orbital population analysis by the NBO 5.0 program.[43] The energy of the $[Ag_8(Se_2PH_2)_6]^{2+}$ fragment (Table 2) has been calculated assuming the geometry it adopts in the optimized structure of $[Ag_8(H)(Se_2PH_2)_6]^{2+}$ and expressed in Table 2 relatively to that of its energy minimum as a free empty cage. The bonding energy between the $[Ag_8(Se_2PH_2)_6]^{2+}$ and H^- fragments (Table 2) is calculated as the difference between the energy of $[Ag_8(H)(Se_2PH_2)_6]^{2+}$ and the sum of the energies of its $[Ag_8(Se_2PH_2)_6]^{2+}$ and H^- fragments. Representation of the molecular structures was done using the program MOLEKEL 4.3.[44] The gauge including atomic orbital (GIAO)[45] method has been used to compute the ^{1}H chemical shifts, $\delta = \sigma_{TMS} - \sigma_{cluster}$, where σ_{TMS} and $\sigma_{cluster}$ are, respectively, the isotropic chemical

(37) Included in *SAINT V4.043*: software for the CCD Detector System; Bruker Analytical: Madison, WI, 1995.

(38) Sheldrick, G. M. *SHELXL-97*: Program for the Refinement of Crystal Structure; University of Göttingen: Göttingen, Germany, 1997.

(39) *SHELXL 5.10* (PC Version): Program Library for Structure Solution and Molecular Graphics; Bruker Analytical: Maidson, WI, 1998.

(40) Frisch, M. J. et al. *Gaussian 03*, revision B.04; Gaussian, Inc.: Pittsburgh PA, 2003.

(41) Perdew, J. P. *Phys. Rev. B* **1986**, *33*, 8822–8824.

(42) Weigend, F.; Ahlrichs, R. *Phys. Chem. Chem. Phys.* **2005**, *7*, 3297–3305.

(43) Glendening, E. D.; Badenhoop, J. K.; Reed, A. E.; Carpenter, J. E.; Bohmann, J. A.; Morales, C. M.; Weinhold, F. Theoretical Chemistry Institute, University of Wisconsin, Madison, WI, 2001; http://www.chem.wisc.edu/~nbo5.

(44) Flukiger, P.; Luthi, H. P.; Portmann, S.; Weber, J. *MOLEKEL 4.3*; Swiss Center for Scientific Computing: Manno, Switzerland, 2000; http://www.cscs.ch/.

(45) (a) London, F. *J. Phys. Radium* **1937**, *8*, 397–409. (b) McWeeny, R. *Phys. Rev.* **1962**, *126*, 1028–1034. (c) Ditchfield, R. *Mol. Phys.* **1974**, *27*, 789–807. (d) Dodds, J. L.; McWeeny, R.; Sadlej, A. J. *Mol. Phys.* **1977**, *34*, 1779–1791. (e) Wolinski, K.; Hinton, J. F.; Pulay, P. *J. Am. Chem. Soc.* **1990**, *112*, 8251–8260.

shielding of ^{1}H in tetramethylsilane and of the encapsulated hydride in the $[Ag_8(H)(Se_2PH_2)_6]^+$ cluster.

Acknowledgment. Financial support from the National Science Council of Taiwan (NSC 97-2113-M-259-007, 98-2911-I-259-002) and from the Institut Universitaire de France (IUF) are gratefully acknowledged. Travel facilities were provided through the French-Taiwanese ORCHID project no. 19667PA.

Supporting Information Available: Crystallographic information for **1** and **2** (CIF), Figures S1− S4, and cartesian coordinates of the optimized model. This material is available free of charge via the Internet at http://pubs.acs.org.